Set-up and validation of numerical modeling techniques to simulate the cold roll forming of martensitic and high strength steel

(Article begins on next page)

Set-up and validation of numerical modeling techniques to simulate the cold roll forming of martensitic and high strength steel

Set-up and validation of numerical modeling techniques to simulate the cold roll forming of martensitic and high strength steel

Edoardo Masoero[1†], Cristiana Delprete[1†], Lorenzo Giorio[2*†], Giacomo Maculotti[3†], Eugenio Brusa[1†], Luca Caneparo[4†]

[1]Department of Mechanical and Aerospace Engineering (DIMEAS), Politecnico di Torino, C.so Duca degli Abruzzi 24, Torino, 10129, Italy.
[2]Department of Applied Science and Technology (DISAT), Politecnico di Torino, C.so Duca degli Abruzzi 24, Torino, 10129, Italy.
[3]Department of Management and Production Engineering (DIGEP), Politecnico di Torino, C.so Duca degli Abruzzi 24, Torino, 10129, Italy.
[4]Department of Architecture and Design (DAD), Politecnico di Torino, C.so Duca degli Abruzzi 24, Torino, 10129, Italy.

*Corresponding author(s). E-mail(s): lorenzo.giorio@polito.it;
Contributing authors: edoardo.masoero@polito.it; cristiana.delprete@polito.it; giacomo.maculotti@polito.it; eugenio.brusa@polito.it; luca.caneparo@polito.it;
†These authors contributed equally to this work.

Abstract

Roll forming is a material processing technology widely used in industry, especially within the automotive production. Resorting to some new materials promotes the innovation in processing techniques, to increase product quality. Therefore, a precise prediction of process outcomes is required. Despite the progress in rolling mill design, a practical modeling approach to investigate shape and geometry of rolled product has been not yet assessed. The highly nonlinear behavior of material motivates setting up either time consuming numerical analyses, or some simplified approaches, still looking poorly reliable. In this paper, a numerical modeling technique aimed at predicting the properties of rolled product more than mill behavior, has been conceived and tested, to allow manufacturer performing a preliminary calibration of product line. Particularly, a real industrial case has been analyzed, by focusing on three roll forming lines, with 'U', 'W' and 'HAT' cross section, respectively. The first two shapes have been exploited to experimentally validate the numerical model. The 'U' line validation performed on the folded edges distance showed a relative systematic deviation of 1.44% and a dispersion of the relative error of **±0.56%**. For the 'W' line, the validation performed on crucial lengths and angles of the cross section exhibited an average relative error of 0.13% and -0.02%, respectively. The validated numerical approach has been exploited to predict the mill performance in manufacturing the 'HAT' profile, still under development. This activity aimed at providing the designer a tool to predict the process performance and assessing the system layout.

Keywords: systems design, cold roll forming, machine design, advanced high strength steel, high-strength low-alloy steel

1 Introduction

The cold roll forming process (CRF) has been applied over last decades to manufacturing of products, whose operational requirements in terms of dimensions are seldom stringent. Recently, the roll forming process has branched out into several variants, such as cold and hot composite roll forming (CHCRF) [1] , micro-roll forming [2], flexible roll forming (FRF) [3–5], incremental shape rolling (ISR) [6–9] and chain-die forming [10, 11]. Their applications include automotive [12] product and several industrial systems [13–15]. Moreover, in metal forming technologies, the rolling mill [16, 17] can exploit now the electric arc furnace [18, 19], instead of some traditional melting processes, to increase the rate of product manufactured per hour. That enhanced the application of roll forming, being currently developing quite rapidly, with appreciable impact upon industry cost and performance. The cold rolling process currently enables the manufacture of a wide range of products, with different cross section geometries [20]. Moreover, there is a wide variety of materials, that can be used in the roll forming process, such as aluminum alloys [21], titanium alloys [22], steel [15], stainless steel (SS) [23], composite material [24] and the advanced high strength steels (AHSS) [25–28].

The design of cold rolling mill somehow rises up from an optimized roll forming process. A requirement induced by energy saving is reaching the product quality and final dimensions with the lowest number of passes [29]. It can be remarked that roll forming is increasingly used in industry, since auxiliary operations, such as punching, welding, clenching, and cutting, can be included within the forming line, increasing the manufacturing process speed and allowing to rely on a single system, which may be inhibited for some other processes.

In the automotive domain, AHSS are increasingly used to meet some stringent emission limits, improving efficiency and safety criteria. Those steels combine high performance with low mass [26, 27, 30]. ~~The~~ AHSS combine the high yield strength with low total elongation, posing the challenge of spring-back effect, in several metal forming processes [31–34]. The spring-back effect must be carefully controlled [35–38] . This requires resorting to higher loads on rolls during roll forming, although

2

the risk of defect nucleation becomes higher [39]. The AHSS exhibit high strength and limited formability, making roll forming through some conventional processes rather difficult [13, 40, 41]. Internal stresses generated in the product section by the forming process [42] may lead to formation of bow (downward or upward), camber (sideways), twist, wave, flare, or spring-back [43–47]. Moreover, the shape of coil can affect the properties of some materials [48]. Particularly, this can become a main issue, since tolerances in the automotive industry are much more restrictive than in other applications, where roll forming is used, being just about a millimeter. It has been empirically verified that those issues can be mitigated by modifying the roller configuration and/or resorting to over-bending. Nevertheless, the effectiveness of those approaches looks not yet optimized [49].

A current need of a manufacturer of cold rolling mill is inherently the possibility of precisely simulating and predicting the process performance, through an effective numerical modeling of the entire line more than of a single cage. The literature have been investigating more deeply the single cage than the whole line, by means of analytical and numerical approaches. Currently, there is no in-depth literature covering the numerical modeling of the entire rolling line, as most of the relevant literature focuses on the rolled section or the rolling process as such. Moreover, it is remarkable that several issues are simultaneously faced by the design activity. The mill manufacturer is responsible for the process performance as well as of the overall safe and controlled operation of the whole production line. The first issue focuses upon dimensions and shape of final product as well as of its properties after treatments. The second one aims at calibrating actions, being exciting vibration and dissipation, to define properly the mill properties of stiffness and damping and its layout [50]. In that sense, numerical modeling often analyses the interaction between roll and product, dealing with the plastic deformation of rolled element, or the actions' path through the rolls, to prevent undesired phenomena, like the chatter and to control the power consumption for sustainability [51, 52].
The finite element method (FE) is herein applied to simulate three roll forming lines, by means of the Hexagon Simufact Forming software [4, 53]. Those superposed and somehow different needs motivate resorting to some complex and time-consuming numerical models, which sometimes require co-simulation between the Finite Element and the Multibody Dynamics approaches. This turns out into a demanding activity of design, in terms of computational effort and rather difficult validation of models. Furthermore, a consolidated selection of software to numerically simulate the behavior of the whole production line is not yet available.
This activity has been performed in tight cooperation with a manufacturer of rolling mill, to validate then the numerical model. This paper applies a strategy of modeling currently exploited in other domains, like the aerospace and automotive engineering, where complexity of simulation is somehow decomposed in some steps, by resorting to a so-called sizing model being then followed by a more detailed analysis of the system dynamics, once that a first layout has been selected [54] .In this case, even the sizing step looks rather difficult, as the need of defining the layout of the whole roll forming line is poorly modeled by an analytical approach. Therefore, that action is done by

resorting to the Finite Element modeling. It is required to introduce some simplifications, which allow investigating with reduced computational effort the layout suitable to properly shape the rolled product, within geometrical and dimensional requirements. In addition, a specific software is exploited to test its capability in replicating the roll forming mill behavior. The validation of proposed approach is even matter of investigation.
A simplified sizing model has been developed by the Finite Elements. It assures a good similarity to the actual system, being suitable to predict the profile shape of rolled product, under some simplifications, which allow simulating the whole production line, with limited computational effort. Particularly, two lines, namely the 'U' and 'W' ones, corresponding to the shape of cross section of product, have been exploited to validate the numerical approachsolution by comparing results to specimens rolled by the real linecomparison with the specimens behavior worked on the real line at factory. According to needs of manufacturer, the same modeling technique has been applied to predict the system behavior to produce a profile looking as 'HAT', being The third line, namely 'HAT', is designed, but not yet built. Numerical simulation in this case is exploited to perform the trade-off of mill layoutTherefore, numerical simulation is contributing to the trade-off activity performed by designer to assess the final layout. Particularly, it could suggest refinements before the line construction. Specimens consist in parts produced and used in the automotive technical domain. The 'U' and 'W' lines work the AHSS 1180DP material, while the 'HAT' line processes the high-strength low-alloy steel (HSLA) CR380LAD.
The study even investigates the performance of the Hexagon Simufact Forming software [4, 53], as an additional goal of the partner rolling mill manufacturer is setting up a suitable tool chain to implement the numerical modeling approach as soon as it could be validated. Validation exploits technical data collected on the real test case. In the meanwhile, some specific strategies have been applied to the FEM modelling to improve numerical convergence and decrease the computational effort. A novelty of this study, for instance, is the use in this context, of a variable density mesh that reduces the computational time without losing accuracy.

2 Materials and Methods

The three roll forming lines that are herein simulated are modeled to reach the most accurate output possible while minimizing the computational effort. Those simplifications are herein described.

2.1 Model boundary conditions

The modeling approach applied to the roll-forming lines here investigated is the same, but those lines are characterized by some differences in their geometries.
The modeling activity is strictly focuses on the profile geometry more than on the material processing based on the mill operation. Consequently, the geometry of rolls and of coil sheet is considered pivotal. Rolls motion and interactions are less investigated in this case. The numerical solution focused primarily on the profile geometry

prediction. Conversely, the calculation of torque applied to rolls, for instance, is omitted, to reduce the computational time. This approach has been clearly required by manufacturer, being prone to exploit different models while addressing different design issues.
This motivation justifies some simplifications. A first one is related to rolls motion, i.e. rolls do not rotate and do not move the sheet, as in reality. Secondly, the sheet moves forwards with respect to rolls, which are assumed to be stationary. Despite that unnatural representation of system operation, the relative motion of bodies is fully represented, at least to investigate the sheet deformation. The aforementioned simplifications surely limit the validity of this model, which precludes the acquisition of specific information on the line, but satisfy the specific needs of manufacturer in terms of profile geometry prediction. By the way, the torque on rolls cannot be easily determined. Consequently, that approach makes it possible to overcome some limitations, caused by a lack of inputs, being obstacles to define an integrated model suitable to predict all the aspects of process behavior.

According to the above-mentioned simplifications some assumptions have been made. The model assumes that rolls are rigid bodies, and thus they do not exhibit any strain. In the literature, this detail is considered poorly relevant for simulation, while it helps in saving computational time [43]. Also, rolls inertia in this analysis has a limited impact on results, because there is no acceleration applied. Friction has been neglected according to Safdarian and Moslemi [55]. Numerical results demonstrate that friction in the roll-strip contact and speed of the roll station do not affect the longitudinal strain of the strip. Nevertheless, incorporating friction into the simulation is matter of investigation in the literature, to calculate the rolls torque, being a critical parameter for the rolling line design as in [56]. Since the rollers do not rotate, it is possible to model only a portion rather than the whole body. This approach is applied in case of the first three to four rolls of the line, to reduce the system complexity. However, subsequent rolls have been modeled by resorting to the complete geometry, to prevent blockages caused by collisions between the roll edges and sheet. The line feed speed has been set at $100\,\mathrm{mm\,s^{-1}}$. This setup is selected as an appropriate average value, directly by the manufacturer. As motion is reversed, i.e. the metal sheet remains stationary while the mill stations with rolls move towards, constraints are more easily applied. The simulation assumes a constant temperature of 20 degrees, which represents the cold roll forming, and there is no heat source during the process, but for friction between surfaces and mechanical bending, which do not affect significantly the mechanical properties of material. The constraints applied to sheet are classified into two types. The first one pertains to nodes of the front and back faces of sheet, along the z-axis, i.e. the direction of rolling. Every elongation of sheet during forming is inhibited, while along the other axes is free. The second type of constraint is applied by introducing some confluence sidebars in the initial part of the line. Their purpose is keeping the sheet's axial direction. and this is achieved through the use of contact and absence of friction. Those convergence bars are only required at the beginning of the line, where they facilitate the convergence of sheet and prevent derailments. Subsequent stations suffer less those problems as the configuration of rollers guarantees the effective conveyance of sheet.

The roll forming process performed by the rolling mills is preliminarily modeled in the Ubeco Profil software. Starting from the final cross section of product, this software allows defining the so-called 'flower pattern'. It includes and describes the sequence of deformed shapes of product, from its initial flat configuration, to final layout.

With regard to the mesh, the sensitivity of element type in the FEA simulation of springback is assessed in [36], proving the 'Solid-shell' (185) element efficient for accurately forecasting the shape of the part. Consequently, the 'Solid-shell' (185) mesh element is selected for all analyses. Particularly, three elements are used to describe the sheet thickness, since they allow localizing properly the neutral axis in bending. Moreover, in crucial areas of product where bending is more effective, the thickness of elements is reduced [57] to improve the accuracy of calculations and their number increased to obtain a finer mesh. The solver used for the simulation is implicit, as is typical of the Finite Element (FE) approach in Simufact Forming (based on MSC Marc). Fixed time steps have been applied according to the tangential speed of rollers and the element size. No mass scaling has been employed, and the "no remeshing" constraint has been explicitly imposed, which is consistent with the low strain conditions, typical of roll forming process and ensures numerical stability without element distortion.

Regarding the sheet modeling, some predefined sheet lengths have been adopted for each production line, tailored to the specific line configuration. Although the final profile has a fixed length, the cutting of the coil can occur at different stages, depending on the line setup. At the beginning of the line, at the end, or particularly in the case of pre-cut blanks on individual sheets processed one by one. To avoid some simulation issues, such as sheet misalignment during roller entry, excessive corner deformation, and numerical singularities, the front edge of sheet has been modeled with a modified geometry. Particularly, the sharp corners have been removed and the sheet thickness locally reduced, creating a region referred to as the "Feed Area." This rounded and thinned leading edge facilitates smoother entry of the sheet into the forming rollers, ensuring both numerical stability and realistic deformation behavior. In some cases, this Feed Area is also meshed more finely than the central body of the sheet to further reduce the risk of simulation failure and improve convergence robustness.

2.2 Sensitivity analysis

A brief sensitivity analysis is conducted on the "U" roll forming line which will be described in depth in section 2.3. This line was selected due to its short length, which results in lower computational cost an important consideration, particularly in industrial contexts where long simulation times can significantly impact productivity and operational expenses. Three different mesh configurations are evaluated to assess their influence on simulation accuracy and computational time:

- Variable density mesh: divided into two zones: a finer mesh in the feed area (5 mm × 3.5 mm) and a coarser mesh in the central body (10 mm × 3.5 mm).
- Medium mesh: uniform size of 5 mm × 3.5 mm across the entire part.
- Fine mesh: fully refined with a resolution of 2.5 mm × 2.5 mm.

All meshes included three elements through the thickness and the length of the sheet of 1300 mm. All simulations were initially performed using the DP1180 steel grade with isotropic material properties. A final simulation were carried out using the variable mesh configuration with anisotropic properties activated, to evaluate the impact of anisotropy on both the results and the computational time. These simulations were performed with a machine equipped with an Intel®Core™ i7-10750H CPU @2.6GHz and 32.0 GB RAM and were conducted on the basis of the same parameters and with the considerations made previously.

2.3 U line

Fig. 1 Real plant of the 'U' line.

The working roll forming industrial line is herein described (Fig. 1)and is the simplest of three lines herein analyzed. In this case, product cross section assumes the so-called 'U' shape, by analogy with that letter. This profile is deeply investigated in the literature with aim of generalizing the approach applied to other shapes and detecting differences and similarities with other techniques [5, 8, 11, 25, 49, 58]. The main focus of the analysis applied to this line is the end-flare effect, with the identification and evaluation of this phenomenon evident in the 'U' cross section. This line includes up to 8 stations, made up of 2 rolls each, for a total of 16 rolls. To reduce the spring-back effect, a calibrator station was added at the end of the rolling line. This addition brings the total number of stations to 9. Rolls are 20, as the added station includes 4 rolls, i.e. 1 up, 1 down and 2 lateral as shown in Figure 2.

The line is modeled in accordance with the following methodology. As previously stated, the initial three rolls have been modeled in a partial manner, whereas the subsequent rolls have been modeled in their entirety. The insertion of confluence sidebars on the sides of the first rolls is necessary to ensure the correct advancement of the sheet. As illustrated in Figure 2, a calibration bar of a semicircular nature is inserted between Rolls 7 and 8. This modification is intended to facilitate the uninterrupted progression of the sheet into Roll 8. These lateral calibrators, when necessary, are

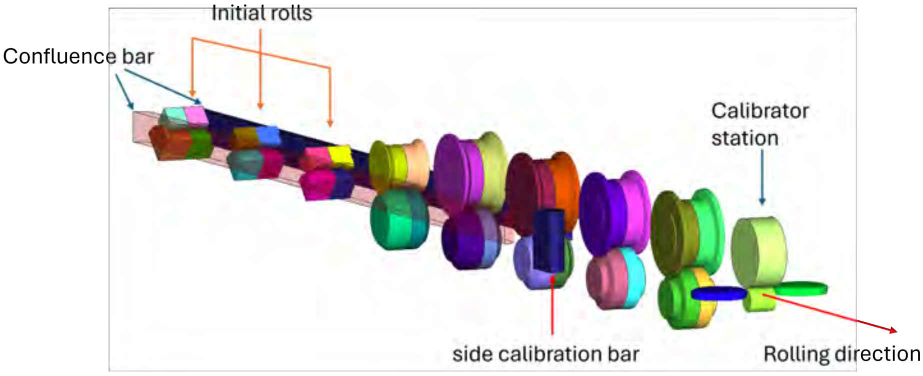

Fig. 2 Model of the 'U' line.

present both in the simulation and in the real line and are essential for the correct profiling process.

Product line in test case works a steel sheet 2235 mm long, 141.46 mm wide and 1.3 mm thick, being obtained by cutting a coil of 1180DP. This steel is an advanced high-strength steel (AHSS) with a dual phase microstructure. It was developed with the specific goal of fulfilling requirements about weight and safety currently faced by the automotive industry and characterized, for instance, by Nimet [27, 59, 60] and the typical chemical composition is shown in Table 1.

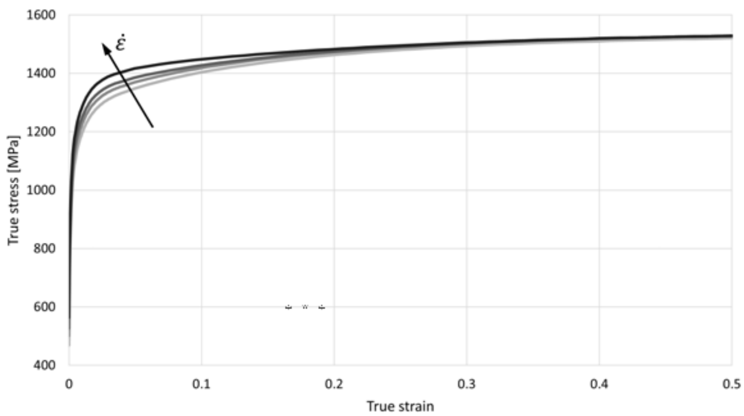

Fig. 3 1180DP true stress/true strain curves at different strain rates [1/s]: ● 0, ● 1, ● 10, ● 100.

In light of the findings from the sensitivity analysis, it was determined that the variable density mesh would be utilized. The mesh was refined in the front part, being known as the 'Feed Area'. The number of elements in the width has been kept constant,

Table 1 Typical chemical composition of an advanced high-strength steel (AHSS) DP1180 with a dual-phase microstructure (values in % by weight) [61].

C %	**Si %**	**Mn %**	**P %**	**S %**	**Al %**	**Nb %**
0.15	0.50	1.50	0.01	0.002	0.04	0.015

while lengthening the elements in the remaining portion of sheet allows maintaining the computational effort acceptable. That mesh allows a considerable reduction in simulation time through two ways. Firstly, it prevents the sheet from becoming stuck in the rolls upon entry, thus obviating the necessity for time-consuming simulations due to blockages. Secondly, the overall calculation time is decreased in comparison to a mesh with constant element size. The average size of finite elements in the feed area is 3.5 mm in width and ~~4 mm in thickness of sheet~~ 5 mm in width of sheet, while 10 mm long elements were used in the central body. Particularly, three elements are used to describe the sheet thickness, since they allow localizing properly the neutral axis in bending. Moreover, in the product's bending zones, where the bending is most pronounced, the thickness of the elements was minimized [57] to approximately 0.5 mm to enhance the precision of the calculations and attain a more refined mesh. The resulting mesh model contains a total of 55,404 elements.

The 1180DP steel, herein tested, is a cold-rolled AHSS, typically selected for automotive applications. Its mechanical properties are illustrated in the true stress/true strain curves at varying strain rates in Fig. 3, being an outcome of some tests performed by the authors at DIMEAS, in the Politecnico di Torino. The aforementioned curves are subsequently incorporated into Simufact, which utilized them for simulation. The software utilizes material data based on the local strain rate that occurs during the simulation, as different strain rates are also available. The greater the number of curves, the greater the representativeness of the material.

2.4 W Line

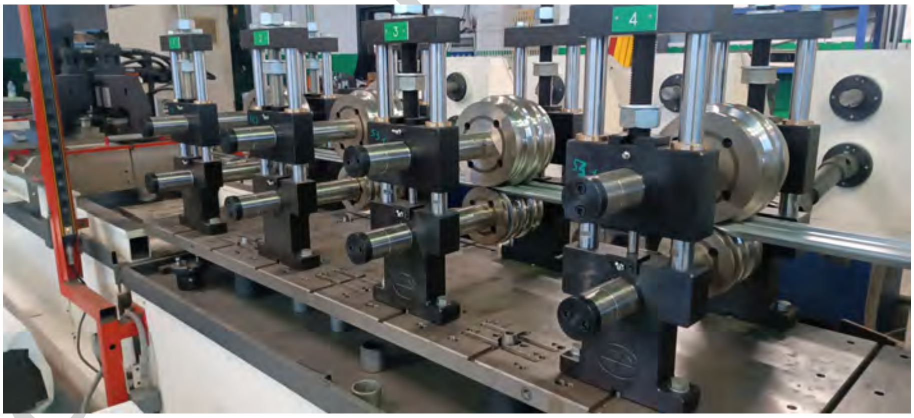

Fig. 4 Real W line plant.

The second line examined looks more complex than the 'U' line and consists of 23 rolls (Fig.4). This 'W' line is a real industrial system, being already in operation. It has been selected to test the software's performance upon a more complex product cross section.

This second line was modeled using the same methodology as it was applied to the first one. Given the low profile of the final section, all rollers have been modeled in a partial manner. The confluence sidebars were also inserted aside the first rollers. Particularly, it this specific configuration required inserting a calibration roller between rollers 18 and 19, as shown in Figure 5.

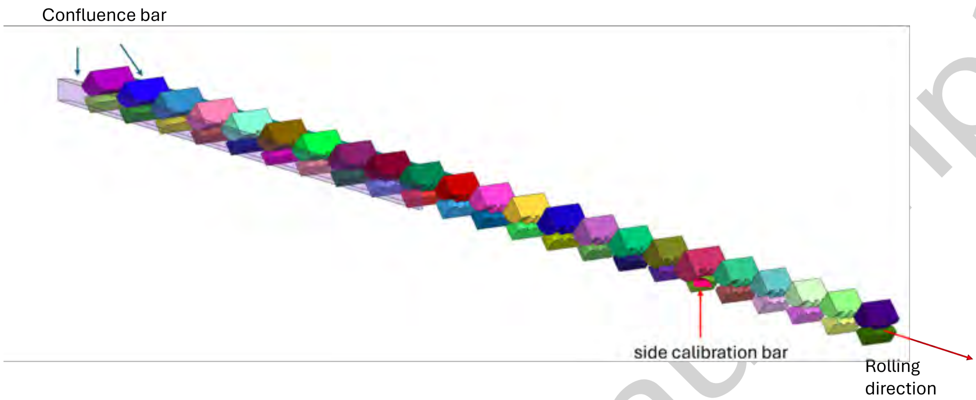

Fig. 5 Model of the W line (on the left) and its real counterpart (on the right).

Figure 6 shows that the cross section shape resembles to the 'W' letter, with some additional folds on the edges. As in previous case, this section is not symmetrical, therefore it was impossible resorting to symmetry functions, to speed up the simulation. The simulation has been carried out on a 'full' sheet to define the correct settings, then a 'pre-cut' sheet has been also used, for both the simulation and the real product line.

The same material 1180DP steel has been investigated as in the 'U' line. Sheet is 650 mm long, 214.4 mm wide, and 1 mm thick. To cope with the increased complexity of the sheet geometry, the mesh has been refined in the front part, being known as the 'Feed Area'.Consequently, the necessity for a compromise between mesh refinement and number of elements has been here circumvented. 2.5 mm by 2 mm elements have been created in the front part, while 10 mm long elements have been used in the central body, and three elements describe the sheet thickness. The mesh includes up to 59,340 elements. As in previous case, the mesh has been refined where bending is more severe. Longer elements in the body of sheet reduces the calculation time, but a very fine mesh in the feed area is essential to prevent errors in the solution, being associated even to element distortion and numerical cancellation.

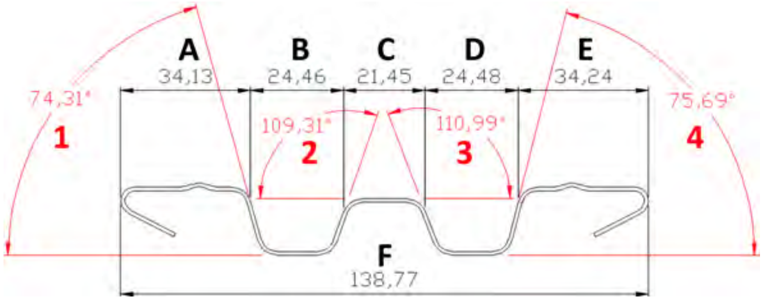

Fig. 6 Reference drawing with measures of the sheet: ● Profile measurements, ● Internal angles.

2.5 HAT line

Fig. 7 Model of the HAT line.

The preliminary activity above described was exploited to predict the system behavior of the third line (Fig. 7) as previous results show a good agreement with real outcomes of process. This line includes 23 stations and 46 rolls. The distance assumed between stations is 500 mm. The new profile, referred to as 'HAT', has been already studied in the literature in some analogous process [6, 8, 10, 58, 62].
Current geometry exhibits an intermediate level of difficulty between the two previous ones. Therefore complexity of simulation does not seem higher than in validated cases and expected errors are at least comparable.

The first four rolls were partially modeled, as 90-degree sectors. The remaining ones were modeled in their entirety. The confluence bars were inserted, while in this case a lateral calibrator between each station was not deemed necessary.

A pre-cut sheet was simulated, with given final geometry, apart from the feed area. This sheet is 2418 mm long, 304.56 mm wide, and 1.5 mm thick. The significant length of this component motivates a greater computational effort. To reduce it, a mesh with variable density was applied, as it had been done for the 'W' line. The mesh includes

10 × 10 mm elements in the central body, while 2.5 × 2.5 mm elements discretize the feed area. In some regions close to folds 2.5 × 2.5 mm and 5 × 5 mm elements were used to precisely predict folding. Three elements were used along thickness. The mesh thus modeled has a total of 108,597 elements.

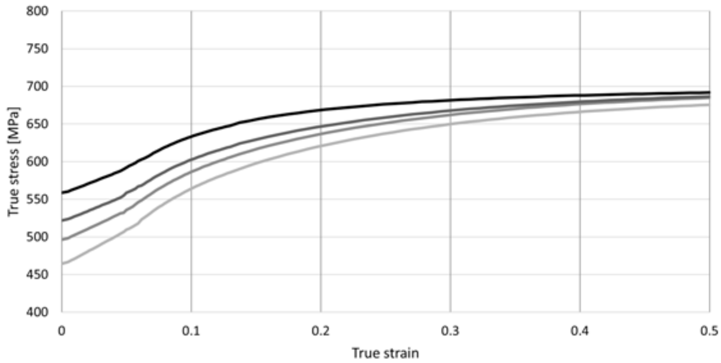

Fig. 8 CR380LA true stress/true strain curves at different strain rates [1/s]: ● 0, ● 1, ● 10, ● 100.

Material used in this simulation is the CR380LAD, i.e. high-strength low-alloy steel (HSLA). These steels exhibit enhanced mechanical properties and corrosion resistance compared to conventional carbon steels. They are highly suitable for cold forming, including bending and molding, while maintaining high strength values. They even allow manufacturing products with complex shapes, being as strong as lightweight, while enabling the use of reduced sheet thicknesses [63, 64]. The stress/strain curves of the CR380LAD (Fig. 8) were obtained as a result of mechanical tests performed by DIMEAS of the Politecnico di Torino and the typical chemical composition in shown in table 2. As was the case for the DP1180, the true stress/true strain curves at varying strain rates were also been incorporated into the simulation.

Table 2 Typical chemical composition of CR380LAD grade according to EN 10268 (in % by weight) [65].

C %	Si %	Mn %	P %	S %	Al %	Ti %	Nb %
≤ 0.12	≤ 0.50	≤ 1.60	≤ 0.030	≤ 0.025	≥ 0.015	≤ 0.15	≤ 0.09

3 Results and discussion

The simulations aimed to reproduce the final profile geometry and common roll-forming defects end flare, spring-back, and twist as accurately as possible. Accurately capturing those defects is critical for predicting material behavior and identifying

design improvements early.
In the first line, the end-flare along the specimen axis was evaluated; in the second one, the spring-back effect was assessed, which affects the final shape and is most pronounced at corners of cross section. Compensation for spring-back via overbending is therefore incorporated into the line design. The third line followed the same rationale, i.e. once spring-back had been estimated, the forming sequence was adjusted to mitigate its effect. Complete elimination of end flare and spring-back remains challenging, and some studies [37] have explored advanced approaches such as machine learning to predict and counteract it.

3.1 Sensitivity analysis

The outcomes of the sensitivity analysis are summarized in Table 3. As shown, the variation in computational time between different mesh configurations is substantial, particularly given the inherently high cost of roll forming simulations. The simulation using the variable mesh required 18.5 hours, while the medium mesh required to 44.5 hours. The fine mesh simulation took the longest, reaching 108 hours. This corresponded to a 484% increase in computational time from the fastest to the slowest configuration.
Regarding the accuracy of the results, all simulations were conducted on the "U" line, using a consistent method of evaluation: the lateral distance between the upper edges of the folded flanges was measured along the full longitudinal profile, as detailed in the following Section 3.2. The average deviation between the variable and medium mesh configurations was 0.89%. Interestingly, the fine mesh did not further improve accuracy; instead, it slightly worsened, with an average error difference of only 0.3% compared to the variable mesh.
Given that the discrepancies between the three mesh configurations remained below 1%, the variable mesh was selected for further simulations. This choice allows for a substantial reduction in computational cost while maintaining acceptable accuracy an especially relevant consideration for longer and more complex lines where time savings are even more pronounced.
As for the material anisotropy, its impact on the results was limited. A simulation incorporating anisotropic properties showed an average deviation of approximately 0.16% compared to the isotropic case, but required an 11% increase in computation time. Based on this trade-off, and the marginal influence on accuracy, anisotropy was excluded from the remaining simulations.

3.2 End-flare analysis of line U

The geometry of the 'U' line is notably quite simple, therefore its examination has been performed to test some operational features of the software. This simple shape makes easier the detection of the so-called end-flare defects, by simulation, and for the experimental validation of model. The end-flare effect is a common defect in roll forming, and can be mainly attributed to residual stress in material resulting from the cutting process [43–45]. Simulation aims at reproducing the defect as accurately as possible, where present, rather than eliminating or mitigating it. The numerical

Table 3 Mesh settings: element size, count, runtime and relative cost

Mesh Type	Variable density	Medium	Fine
Elem. size (mm)	$5\backslash10 \times 3.5$	5×3.5	2.5×2.5
Elem. in thickness	3	3	3
Elem. count	32562	63180	159120
Time (hour)	18.5	44.5	108
Time incr.	–	141%	484%
Relative Err.(Avg)	–	0.89%	0.30%

results obtained for 'U' is illustrated in Figure 9. In the image it is possible to observe how the data of the simulation were collected.

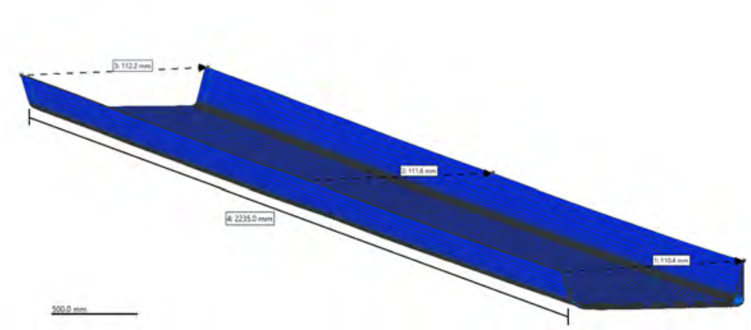

Fig. 9 Simulation results for the U line. The measurements indicate the distance between the tip of the two folded flaps.

Results look promising in terms of effective prediction of the real product behavior. Particularly, to ascertain the accuracy of those results, a comparison has been completed with the actual geometry of the real component. The experimental measurements have been performed with a Mitutoyo Digital AOS ABS Caliper model 500-182-30, with a resolution of 0.01 mm and, in accordance with the standard ISO 13385-1:2019 [66], a Maximum Permissible Error for the partial surface contact error, $E_{MPE} = \pm 0.02$ mm.The distance between the two folded edges of sheet has been selected as crucial measurement for that validation. That choice allows basing the validation activity upon a measurement easier and faster than measuring angles, which could potentially introduce greater errors. Moreover, this verification method is currently applied by the company.

The measurements upon the specimen have been taken approximately every 100 mm of length, leading to a total number of 23 equally spaced points. Nevertheless, the simulation outcomes includes 251 measured points, considering nodes present within the mesh. Figure 10 shows a comparison of simulation and experimental tests results, respectively, for the real sheet worked. It is evident that the end-flare effect is present, in both the simulation and direct measurement. Particularly, along the profile it can be remarked that the lead end is more closed than in the central part of body, while the tail end is more open. This phenomenon is prevalent in roll forming and is primarily attributed to residual stress occurring in the material under cutting [43, 44].

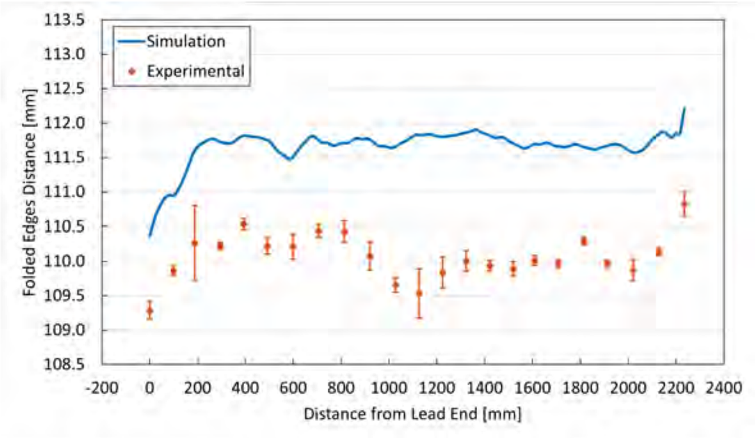

Fig. 10 End flare, real vs simulation: ● Experimental Measurement average, ▬ Simulation. The distance between the edges, measured as illustrated in Figure 9, is presented in the graph along the entire length of the specimen to evaluate the end-flare effect.

The simulation accurately predicts the distance between the two folded edges along the entire length of sheet in operation, as well as the corresponding distance between the two folded edges along the entire length. As shown in Figure 10, the simulation results are affected by a statistically significant systematic error of 1.58 mm, representing a relative systematic error of 1.44%, which is considered compatible with the typical application of this modeling activity in the industrial context, and explainable with an imperfect knowledge of the elastic properties of the material. The dispersion of the error, corrected for the systematic bias, can be evaluated combining also the accuracy and resolution of the measuring instrument as ± 0.62 mm at a 95% confidence level, i.e. $\pm 0.56\%$ in terms of relative error.

The errors that have been identified may be attributable to a variety of factors. Primarily, they may be attributed to the material utilized in the actual line in comparison to the material inputted in the simulation, which is uncoated. Regrettably, the authentic material with the authentic coating could not be characterized, and consequently, an uncoated version was characterized. It is acknowledged that the material's characteristics exhibit slight variations between batches. Consequently, this aspect could be a contributing factor to the observed phenomenon. Certainly, being a simplified model of the line, the result can also suffer from these approximations. Finally the type of mesh can influence the results obtained and have a significant impact on the resultant outcomes. Use of a finer mesh may potentially yield enhanced results in this instance. However, it should be noticed that this would necessitate an extensive calculation time, which is not commensurate with industry standards and needs.

3.3 Shape analysis of line W

The simulation has been validated by comparing numerical results to measurements performed upon a real specimen work by the roll forming line of previous case (Fig.11). The roll formed specimen has been measured with a laser scanner API iScan3D (associated to a laser tracker API Radian R-20) calibrated with flatness error of 41 µm and calibrated length error of 20 µm [67]. Figure 12 (left) shows the laser scanning process at DIGEP (dept. of Management and Production Eng.) Lab of the Politecnico di Torino, resulting in the point cloud (right) used for measurements. A number of edges equal to 6 has been selected for validation, from A to F, and 4 angles of the central body (Fig. 6). The edges and angles selected for comparison have been chosen according to their significance with regard to the geometry of component.

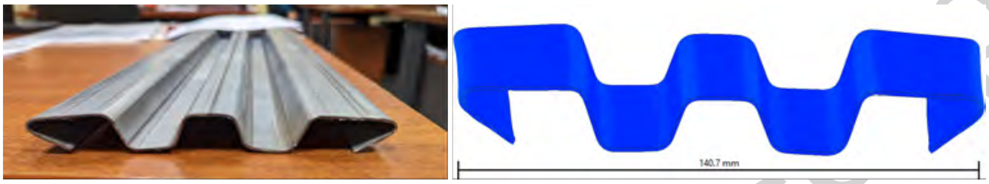

Fig. 11 Cross section of the roll formed sheet, real (left) and simulation (right).

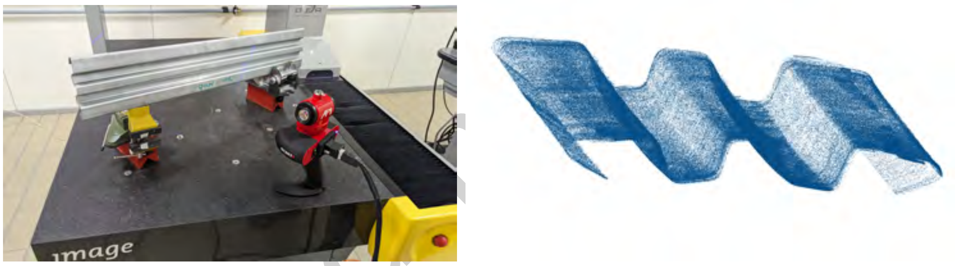

Fig. 12 Specimen with 3D laser scan used for measurements carried out (left) and point cloud obtained from the measurements (right).

The upper parts of Tables 4 and 5, display the measurements of the three elements: nominal dimension from CAD, simulation results, and real component(specimen). The lower part of those tables displays the relative error between simulation and measurement.
Upon examination of the error in measurements, it is evident that matching between simulation and real body is highly accurate, particularly in regard to edges, where the closer the value is to zero, the better the closeness in agreement. The simulation provides measurements that differ by an error of (0.037 ± 0.532) mm, i.e. 0.13% in terms of relative error. The dispersion reports the measurement uncertainty evaluated combining the reproducibility with the accuracy of instrument at a 95% confidence level

Table 4 Measures of the sheet of the W line – edge measurements; segments A through F are indicated in Figure 6.

	A	B	C	D	E	F
CAD Design [mm]	34.13	24.46	21.45	24.48	34.24	138.77
Simulation [mm]	34.60	25.25	21.04	26.24	33.97	140.70
Real (specimen) [mm]	34.50	24.91	20.97	26.39	34.21	140.60
Relative Error [%] (Sim/Real)	0.29	1.36	0.33	-0.57	-0.70	0.07

Table 5 Measures of the sheet of the W line - Angle measurements. Angle 1 through 4 are indicated in Figure 6.

	1	2	3	4
CAD Design [deg]	74.31	109.31	110.99	75.69
Simulation [deg]	72.79	109.15	111.42	77.01
Real (specimen) [deg]	75.45	109.36	109.67	75.47
Relative Error [%] (Sim/Real)	-3.53	-0.19	1.60	2.04

[68–70]. The error shows a maximum magnitude of 1.36% and a minimum magnitude of 0.07%.

Considering the angles, the relative error between simulation and specimen is approximately -0.02%, with a maximum magnitude of 3.53% (angle 1) and a minimum magnitude of 0.19% (angle 2). The error on the angle shows an asymmetry, and a value of $(0.105 \pm 6.5)^{\circ}$, reporting a confidence interval at 95% confidence level evaluated from the reproducibility.

Those results demonstrate that both the edge and angle numerical results exhibit a satisfactory approximation of measurements. Particularly, a preliminary hypothesis about test on the mean for both the length and angular error values shows that the error cannot be considered systematic with a risk of error of 5%, reporting respectively a p-value of 0.43 and 0.49.

3.4 Shape analysis of line HAT

Figure 13 illustrates the final outcome of the last simulation.

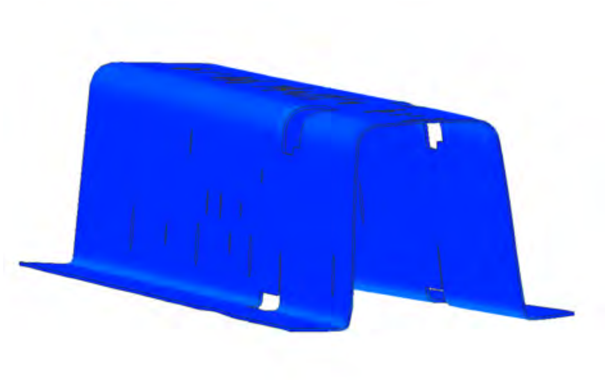

Fig. 13 Simulation results for the HAT line.

Figure 14 investigates the accuracy of overlap between the simulation model and the CAD 3D geometry. The top figure compares the superposed geometries, whereas the last plot in sequence identifies the discrepancy between the simulation and CAD model respectively. From left to right, those images depict the front and back of component. The so-called 'feed areas' have been omitted. They do not align with the actual component, although they cover a minor surface. Figure 14 clearly reveals the presence of a twist deformation, a common phenomenon in roll forming processes. The measured twist angle, defined as the angular offset between the front and rear cross sections, is approximately 3.93°. Although relatively small, this twist is consistent with observations on physical parts and is considered realistic by the manufacturer. In this specific case, the deformation may be correctable in the post-processing stage without requiring a redesign of the forming rolls. However, in other applications or for more severe twisting, it may become necessary to adjust the roll geometry to introduce compensation directly during the forming process.Figure 14 demonstrates that a twist effect holds, being a common phenomenon in roll forming. The offset of the front and rear cross sections has been measured, resulting in a twist angle of 3.93°. This is a realistic outcome, according to manufacturer. It can be considered during the design activity and to introduce some compensations.

Figure 15 investigates the overlap between the simulation and the reference geometry, respectively. Particularly, angles in the simulation results have been evaluated and compared to those of the reference CAD model. The four angles analyzed are numbered in Figure 15.

To account for the variability in measurements due to the end-flare and twist effect, respectively, as well as for other potential sources of variation, the measurements have been taken at three different positions on sheet. Particularly, they have been taken at middle region (50% of length) and at two ends (10% and 90% of length). It can be remarked that a distance of 10% of length has been left from real edges to circumvent any potential errors resulting from the inlet and exit of rollers, since deformations due to contact with rollers or singularities in the mesh could be present.

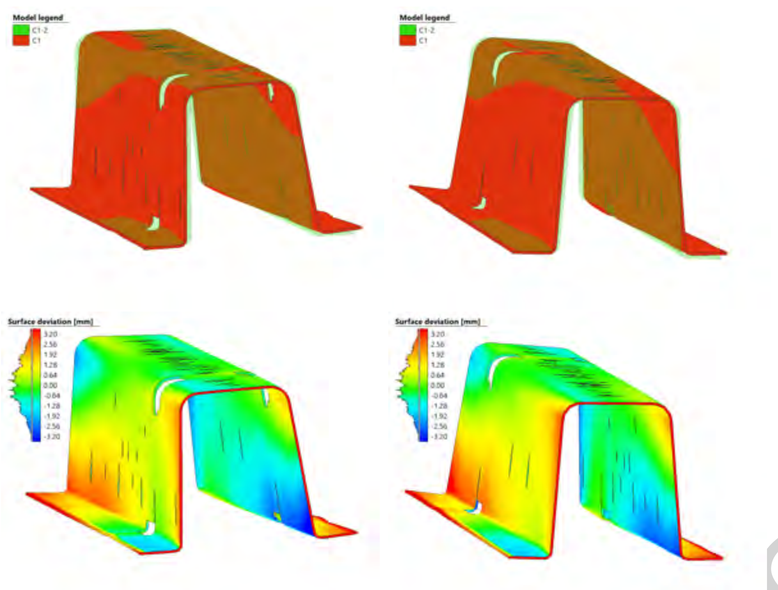

Fig. 14 Simulation compared to CAD 3D geometry: simulated component (red) and CAD reference (transparent green).

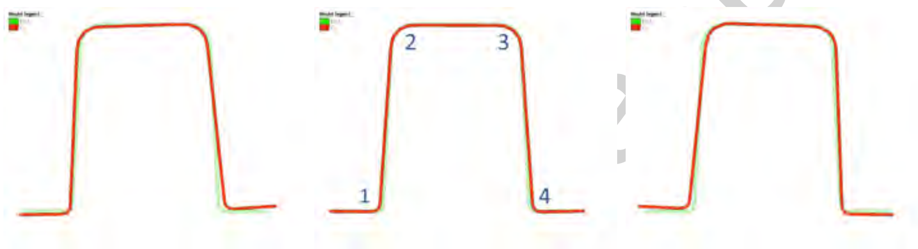

Fig. 15 Overlap of the simulated geometry (red) with the reference geometry (green) at 90%, 50% and 10% of the total length, respectively. The numbers indicate the angles examined.

The four angles of the cross section previously identified have been measured at the beginning (front), at the center (middle) and at the end (back) of the metal sheet. Those measurements have been then compared to values of the reference angles of the CAD design.
Table 6 includes the values of each angle for the three sections above mentioned, along with values of the reference section and corresponding relative error between simulation and reference values. It can be appreciated that the simulation data are in close agreement with the reference data, with the relative error from 1.80% to 0.11% (with an average of 0.82%). The relative error has been averaged across each angle, yielding the following deviations −0.41%, −1.12%, −1.541%, and −0.20%, respectively. As previously mentioned, corners suffer the springback effect. It is evident that the utilization of materials akin to those employed in these cases serves to exacerbate the

issue. Nevertheless, by employing a methodology that entails the prediction of material behavior, intervention becomes a possibility, with the potential for enhancement through slight overbending, thereby ensuring optimal outcomes. The measurements taken at the back, middle, and front locations of sheet indicate slightly narrower angles than designed, with a slight discrepancy between the simulation data and the reference values. However, the average deviation for each section is relatively minor.

Table 6 Measurements of the four angles of the section and their relative errors compared to the CAD design.

Pos.	CAD [deg]	Simulation [deg]			Rel. Err. [%]		
		Back	Middle	Front	Back	Middle	Front
1	87	86.67	86.64	86.63	−0.38	−0.42	−0.43
2	87	86.05	86.18	85.89	−1.10	−0.95	−1.29
3	87	85.91	85.76	85.46	−1.27	−1.45	−1.80
4	87	86.92	87.10	87.51	−0.09	0.11	0.58

4 Conclusion

This study copes with the lack of a numerical modeling approach suitable to support the roll forming line designer during a preliminary trade-off activity of system layout, being mainly based upon the material process performance and related to the precise shape and geometry of rolled product. Several models are already available in the literature to investigate the whole rolling mill system behavior, being especially focusing on actions and control of the roll forming line. However, time consumption and cost of analyses look unsuitable to perform a calibration of the whole plant layout, in terms of preliminary trade-off. A different approach, mainly based upon the numerical modeling of roll forming in terms of product layout, has been proposed, implemented and tested. Some limitations do not allow using the same model for a deeper design synthesis of the mill structure, but once that layout has been defined, it allows proceeding faster and straight to final assessment. Particularly, an industrial test case has been exploited to implement a complete modeling activity, to set up the numerical model, being then experimentally validated. Once that numerical model demonstrates to be effective, it is further and successfully used to reconfigure the rolling mill layout for a new product, with different shape and geometry, not yet produced.

Matter of discussion for numerical model validation is the accuracy in predicting the shape of cross section of sheet at the end of process. The study proceeded with a first sheet profile, namely 'U', to set up the model. An assessment has been performed in case of a second profile, i.e. the 'W', being more difficult to be manufactured, because of angles and springback effects, to finally exploit the validated model to predict the system performance, in case of the 'HAT' configuration.

- In case of the so-called 'U' profile, an accurate approximation of the actual cross section has been found, despite a systematic mean deviation of 1.58 mm which has been observed over the entire length of production line. It has been likely attributed to some parameters that cannot be fully identified, accounting for a relative systematic error of 1.44%. The dispersion of the error corrected for the systematic bias allowed reaching a relative error in results of $\pm 0.56\%$.
- The 'W' line exhibits within the cross section some crucial lengths and angles, to be carefully checked in validation. They exhibited an average relative error of 0.13% upon lengths and of -0.02% upon angles.

The validated model has been then applied to predict the performance of a new roll forming line, to produce the so-called 'HAT' profile. This has not been built yet, but the model allowed defining layout of rolls, shapes and sizes compatible with product geometry and tolerances.

The study demonstrates that, under some simplifications, the computational effort just required for a preliminary calibration of the roll forming line to define the system layout, for given product shape, is effective and allow balancing the lower computational effort with the limited validity of outcomes, being reliable in terms of product layout, and incomplete about details about the mill dynamics.

- To reach that result it can be remarked that the study even investigated critical issues and mitigations to be applied to the numerical model. Particularly, to mitigate errors in layout angles, some options in the finite elements model were even tested, always keeping the computational effort as low as possible. Use of a variable-length mesh, for instance, exhibited favorable results, as well as reduction of number of elements in some regions of numerical model does not significantly affect accuracy of results, while keeping computational effort in solution sustainable. Moreover, a fine mesh in some regions is required to avoid blockages issues, while coarse mesh applied to regions less stressed, helps in reducing the computational time.
- Uncoupling sizing from detailed steps of modeling of the roll forming design looks a successful strategy to decompose the complexity traditionally associated to that system.
- Simplifications applied, modeling approaches and strategies in meshing allows setting up a numerical model which looks suitable for a preliminary definition of the layout of roll forming line along the trade-off analysis, as a sizing step of the whole product line development, while a deeper assessment is then required and performed, more easily and somehow faster, by focusing upon critical issues and details, being explored by some specific numerical models, often more expensive in terms of computational effort.

Acknowledgments

The authors thank Coproget s.r.l. company for the availability of the roll forming lines and the alloys used in the study.

Declarations

- Funding: This work was supported by the Call IR2 of the Piedmont Region of Italy, Grant 309-56.
- Competing interests: The authors have no relevant financial or non-financial interests to disclose.
- Ethics approval and consent to participate: Not applicable.
- Consent for publication: Not applicable.
- Data availability: The data are available from the authors upon reasonable request.
- Code availability: Not applicable.
- Author contribution: The authors contributed equally to the writing of the article.

References

[1] Wang, Y., Mehari, Z.A., Wu, J., Han, J.: Optimization design of process parameters for cold and hot composite roll forming of the AHSS square tube using response surface methodology. The International Journal of Advanced Manufacturing Technology **123**(1), 527–542 (2022) https://doi.org/10.1007/s00170-022-10119-0

[2] Abeyrathna, B., Zhang, P., Pereira, M.P., Wilkosz, D., Weiss, M.: Micro-roll forming of stainless steel bipolar plates for fuel cells. International Journal of Hydrogen Energy **44**(7), 3861–3875 (2019) https://doi.org/10.1016/j.ijhydene.2018.12.013

[3] Kasaei, M.M., Naeini, H.M., Abbaszadeh, B., Silva, M.B., Martins, P.A.F.: Flexible roll forming. In: Davim, J.P. (ed.) Materials Forming and Machining. Woodhead Publishing Reviews: Mechanical Engineering Series, pp. 51–71. Woodhead Publishing, Sawston, UK (2015). https://doi.org/10.1016/B978-0-85709-483-4.00003-X

[4] Sreenivas, A., Abeyrathna, B., Rolfe, B., Weiss, M.: Longitudinal strain and wrinkling analysis of variable depth flexible roll forming. Journal of Manufacturing Processes **81**, 414–432 (2022) https://doi.org/10.1016/j.jmapro.2022.06.063

[5] Sheu, J.-J., Liang, C.-F., Yu, C.-H., Hsu, W.-C., Lee, P.-K.: Flexible roll forming of U-section product with curved bending profile using advanced high strength steel. Procedia Manufacturing **15**, 782–787 (2018) https://doi.org/10.1016/j.promfg.2018.07.321

[6] Essa, A., Abeyrathna, B., Rolfe, B., Weiss, M.: Prototyping of straight section components using incremental shape rolling. The International Journal of Advanced Manufacturing Technology **121**(5), 3883–3901 (2022) https://doi.org/10.1007/s00170-022-09600-7

[7] Essa, A., Abeyrathna, B., Rolfe, B., Weiss, M.: Flange wrinkling in incremental shape rolling. In: Materials Research Proceedings, vol. 28, pp. 1047–1056.

Association of American Publishers, AGH University of Science and Technology, Kraków, Poland (2023). https://doi.org/10.21741/9781644902479-115

[8] Essa, A., Abeyrathna, B., Rolfe, B., Weiss, M.: Incremental shape rolling of top-hat shaped automotive structural and crash components. Journal of Materials Processing Technology **321**, 118162 (2023) https://doi.org/10.1016/j.jmatprotec.2023.118162

[9] Essa, A., Abeyrathna, B., Rolfe, B., Weiss, M.: Incremental shape rolling of a variable depth profile. Journal of Materials Processing Technology **316**, 117964 (2023) https://doi.org/10.1016/j.jmatprotec.2023.117964

[10] Liang, Z., Zou, T., Dai, W., Zhang, Z., Liu, Y., Lu, K., Li, D., Ding, S., Peng, Y.: Compensate for longitudinally discrepant springback and bow in chain-die forming processes by multiple sections optimization. The International Journal of Advanced Manufacturing Technology **121**(9), 6407–6430 (2022) https://doi.org/10.1007/s00170-022-09728-6

[11] Li, Y., Liang, Z., Zhang, Z., Zou, T., Li, D., Ding, S., Xiao, H., Shi, L.: An analytical model for rapid prediction and compensation of springback for chain-die forming of an AHSS U-channel. International Journal of Mechanical Sciences **159**, 195–212 (2019) https://doi.org/10.1016/j.ijmecsci.2019.05.046

[12] Sedlmaier, A., Dietl, T.: 3D roll forming center for automotive applications. Procedia Manufacturing **15**, 767–774 (2018) https://doi.org/10.1016/j.promfg.2018.07.319

[13] Abeyrathna, B., Rolfe, B., Weiss, M.: The effect of process and geometric parameters on longitudinal edge strain and product defects in cold roll forming. The International Journal of Advanced Manufacturing Technology **92**(1), 743–754 (2017) https://doi.org/10.1007/s00170-017-0164-x

[14] Bui, Q.V., Boman, R., Papeleux, L., Wouters, P., Kergen, R., Daolio, G., Duroux, P., Flores, P., Habraken, A., Ponthot, J.-P.: Springback and twist prediction of roll formed parts. In: IDDRG 2006 International Deep Drawing Research Group, Drawing the Things to Come, Trends and Advances In Sheet Metal Forming, Porto, Portugal (2006)

[15] Teixeira, R.L.P., de Lacerda, J.C., Florencio, K.C., da Silva, S.N., Henriques, A.B.: TRIP effect produced by cold rolling of austenitic stainless steel AISI 316L. Journal of Materials Science **58**(7), 3334–3345 (2023) https://doi.org/10.1007/s10853-023-08235-7

[16] Brusa, E., Lemma, L.: Numerical and experimental analysis of the dynamic effects in compact cluster mills for cold rolling. Journal of Materials Processing Technology **209**(5), 2436–2445 (2009) https://doi.org/10.1016/j.jmatprotec.2008.05.044

[17] Brusa, E., Lemma, L., Benasciutti, D.: Vibration analysis of a Sendzimir cold rolling mill and bearing fault detection. Proceedings of the Institution of Mechanical Engineers, Part C: Journal of Mechanical Engineering Science **224**(8), 1645–1654 (2010) https://doi.org/10.1243/09544062JMES1540

[18] Brusa, E., Franceschinis, E., Morsut, S.: Compact Modelling of Electric Arc Furnace Electrodes for Vibration Analysis, Detection and Suppression. CMES - Computer Modeling in Engineering and Sciences **42**(2), 75–106 (2009)

[19] Brusa, E., Morsut, S.: Design and Structural Optimization of the Electric Arc Furnace Through a Mechatronic-Integrated Modeling Activity. IEEE/ASME Transactions on Mechatronics **20**(3), 1099–1107 (2015) https://doi.org/10.1109/TMECH.2014.2364392

[20] Yan, Y., Wang, H., Li, Q., Qian, B., Mpofu, K.: Simulation and experimental verification of flexible roll forming of steel sheets. The International Journal of Advanced Manufacturing Technology **72**(1), 209–220 (2014) https://doi.org/10.1007/s00170-014-5667-0

[21] Suckow, T., Schroeder, J., Groche, P.: Roll forming of a high strength AA7075 aluminum tube. Production Engineering **15**(3), 573–586 (2021) https://doi.org/10.1007/s11740-021-01046-2

[22] Badr, O.M., Rolfe, B., Weiss, M.: Effect of the forming method on part shape quality in cold roll forming high strength Ti-6Al-4V sheet. Journal of Manufacturing Processes **32**, 513–521 (2018) https://doi.org/10.1016/j.jmapro.2018.03.022

[23] Wang, J., Liu, H.-M., Li, S.-F., Chen, W.-J.: Cold Roll Forming Process Design for Complex Stainless-Steel Section Based on COPRA and Orthogonal Experiment. Materials **15**(22), 8023 (2022) https://doi.org/10.3390/ma15228023

[24] Qi, R., Sun, S., Yan, S.: Numerical investigation of cold roll-forming process for three-layer metal sheets and al/abs/al composites. International Journal of Steel Structures **25**(2), 338–349 (2025) https://doi.org/10.1007/s13296-025-00935-x

[25] Lindgren, M.: Cold roll forming of a U-channel made of high strength steel. Journal of Materials Processing Technology **186**(1), 77–81 (2007) https://doi.org/10.1016/j.jmatprotec.2006.12.017

[26] Joo, B., Lee, H., Kim, D., Moon, Y.: A Study on Forming Characteristics of Roll Forming Process with High Strength Steel. In: AIP Conference Proceedings, vol. 1383. Seoul, Korea, pp. 1034–1040 (2011). https://doi.org/10.1063/1.3624622

[27] Zhao, J., Jiang, Z. (eds.): Rolling of Advanced High Strength Steels: Theory, Simulation and Practice. CRC Press, Boca Raton, FL, USA (2017). https://doi.org/10.1201/9781315120577

[28] Taylor, T.: Novel cold-rolled martensitic ultra-high-strength steels for roll forming technologies. Materials Science and Technology **32**(16), 1730–1741 (2016) https://doi.org/10.1080/02670836.2016.1146840

[29] Ferreira, P.B.F.: Roll Forming - A Study on Machine Deflection by Means of Experimental Analysis and Numerical Developments. Master's thesis, Universidade do Porto (Portugal), Porto, Portugal (2016). https://repositorio-aberto.up.pt/bitstream/10216/83319/2/125908.pdf

[30] Aldanondo, E., Taboada, A., Arruti, E., Alvarez, P., Echeverria, A.: Friction stir spot welding of DP1200 steel. In: Fujii, H. (ed.) Proceedings of the 1st International Joint Symposium on Joining And Welding, pp. 179–182. Woodhead Publishing, Osaka, Japan (2013). https://doi.org/10.1533/978-1-78242-164-1.179

[31] Lu, Z., Li, D., Cao, L., Cui, H., Xu, J.: Springback Control in Complex Sheet-Metal Forming Based on Advanced High-Strength Steel. Coatings **13**(5), 930 (2023) https://doi.org/10.3390/coatings13050930

[32] Bene, F.F.M., Liang, Z.Y., Yang, H., Li, D.Y., Ding, S.C.: Finite Element Study on Chain-Die Forming of an AHSS Channel with Variable Depth. IOP Conference Series: Materials Science and Engineering **727**(1), 012012 (2020) https://doi.org/10.1088/1757-899X/727/1/012012

[33] Abeyrathna, B., Rolfe, B., Hodgson, P., Weiss, M.: Local deformation in roll forming. The International Journal of Advanced Manufacturing Technology **88**(9), 2405–2415 (2017) https://doi.org/10.1007/s00170-016-8962-0

[34] Salonitis, K., Paralikas, J., Chryssolouris, G.: Roll Forming of AHSS: Numerical Simulation and Investigation of Effects of Main Process Parameters on Quality. In: Pantelakis, S., Rodopoulos, C. (eds.) Engineering Against Fracture. Proceedings of the 1st Conference, pp. 327–336. Springer, Patras, Greece (2009). https://doi.org/10.1007/978-1-4020-9402-6_26

[35] Liu, X.-l., Cao, J.-g., Huang, S.-x., Yan, B., Li, Y.-l., Zhao, R.-g.: Experimental and numerical prediction and comprehensive compensation of springback in cold roll forming of UHSS. The International Journal of Advanced Manufacturing Technology **111**(3), 657–671 (2020) https://doi.org/10.1007/s00170-020-06133-9

[36] Liu, X., Cao, J., Chai, X., Liu, J., Zhao, R., Kong, N.: Investigation of forming parameters on springback for ultra high strength steel considering Young's modulus variation in cold roll forming. Journal of Manufacturing Processes **29**, 289–297 (2017) https://doi.org/10.1016/j.jmapro.2017.08.001

[37] Cu, S., Sun, Y., Wu, K.: Machine learning methods for springback control in roll forming. International Journal of Material Forming **18**(1), 1–15 (2025) https://doi.org/10.1007/s12289-024-01872-6

[38] Wang, R., Sun, C., Liu, X., Li, S., Su, C., Huang, J., Bai, Z.: Research on springback mechanism of ta2/q235b composite plate in roll forming. Journal of Manufacturing Processes **119**, 715–728 (2024) https://doi.org/10.1016/j.jmapro.2024.03.104

[39] Asgari, A., Pereira, M., Rolfe, B., Dingle, M., Hodgson, P.: Design of experiments and springback prediction for AHSS automotive components with complex geometry. In: AIP Conference Proceedings, vol. 778. Detroit, MI, USA, pp. 215–220 (2005). https://doi.org/10.1063/1.2011220

[40] Abeyrathna, B., Ghanei, S., Rolfe, B., Taube, R., Weiss, M.: Springback and end flare compensation in flexible roll forming. IOP Conference Series: Materials Science and Engineering **967**(1), 012048 (2020) https://doi.org/10.1088/1757-899X/967/1/012048

[41] Wei, Z., Cao, J., Cheng, J., Wang, X., Zhu, H., Zhu, X., Zhao, R.: Precise local deformation control for uhss thin-walled component in roll forming. Journal of Manufacturing Processes **112**, 302–312 (2024) https://doi.org/10.1016/j.jmapro.2024.01.017

[42] Díaz, A., Cuesta, I.I., Alegre, J.M., de Jesus, A.M.P., Manso, J.M.: Residual stresses in cold-formed steel members: Review of measurement methods and numerical modelling. Thin-Walled Structures **159**, 107335 (2021) https://doi.org/10.1016/j.tws.2020.107335

[43] Halmos, G.T. (ed.): Roll Forming Handbook. CRC Press, Boca Raton (2005). https://doi.org/10.1201/9781420030693

[44] Moneke, M., Groche, P.: The origin of end flare in roll formed profiles. International Journal of Material Forming **14**(6), 1439–1461 (2021) https://doi.org/10.1007/s12289-021-01640-w

[45] Zou, T., Liu, Y., Tang, W., Li, D.: Analysis and Suppression of End Flare in AHSS Roll-Formed Seat Rail. Automotive Innovation **6**(3), 404–413 (2023) https://doi.org/10.1007/s42154-023-00240-5

[46] Wang, Y., Xu, X., Ren, B., Liu, J., Zhao, R.: Effect of Geometrical Factors on Torsion in Cold Roll Forming of the Lower Side Beam of a Car. Applied Sciences **11**(17), 7852 (2021) https://doi.org/10.3390/app11177852

[47] Liang, C., Li, S., Liang, J., Li, J.: Method for Controlling Edge Wave Defects of Parts during Roll Forming of High-Strength Steel. Metals **12**(1), 53 (2022) https://doi.org/10.3390/met12010053

[48] Weiss, M., Abeyrathna, B., Rolfe, B., Abee, A., Wolfkamp, H.: Effect of coil set on shape defects in roll forming steel strip. Journal of Manufacturing Processes **25**, 8–15 (2017) https://doi.org/10.1016/j.jmapro.2016.10.005

[49] Shirani Bidabadi, B., Moslemi Naeini, H., Safdarian, R., Barghikar, H.: Investigation of over-bending defect in the cold roll forming of U-channel section using experimental and numerical methods. Proceedings of the Institution of Mechanical Engineers, Part B: Journal of Engineering Manufacture **236**(10), 1380–1392 (2022) https://doi.org/10.1177/09544054221076628

[50] Wang, J., Brusa, E., Peng, Y., Zhao, X., Wang, M., Delprete, C., Gastaldi, C.: Dynamics and stability analysis of rolling mill system during variable gauge rolling. Meccanica **58**(12), 2439–2454 (2023) https://doi.org/10.1007/s11012-023-01735-5

[51] Wang, J., Zhao, X., Brusa, E., Delprete, C., Hou, X., Xiang, X., Wang, C., Peng, Y.: Stability analysis of rolling mill system for flexible rolling process based on maximum lyapunov exponent. International Journal of Non-Linear Mechanics **166**, 104874 (2024) https://doi.org/10.1016/j.ijnonlinmec.2024.104874

[52] Wang, J., Brusa, E., Peng, Y., Delprete, C., Zhao, X., Xiang, X., Hou, X.: On the effect of vertical motion of roll system upon dynamic behavior and stability of rolling mill. Meccanica **60**(1), 73–93 (2025) https://doi.org/10.1007/s11012-024-01917-9

[53] Zeng, G., Lai, X.-m., Yu, Z.-q., Lin, Z.-q.: Numerical Simulation and Sensitivity Analysis of Parameters for Multistand Roll Forming of Channel Section With Outer Edge. Journal of Iron and Steel Research International **16**(1), 32–37 (2009) https://doi.org/10.1016/S1006-706X(09)60007-8

[54] Delprete, C., Dagna, A., Brusa, E.: Model-based design of aircraft landing gear system. Applied Sciences **13**(20), 11465 (2023) https://doi.org/10.3390/app132011465

[55] Safdarian, R., Moslemi Naeini, H.: The effects of forming parameters on the cold roll forming of channel section. Thin-Walled Structures **92**, 130–136 (2015) https://doi.org/10.1016/j.tws.2015.03.002

[56] Galdos, L., Ulibarri, U., Gil, I., Ortubay, R., Argandoña, E.S.: Friction Coefficient Identification in Roll Forming Processes. Key Engineering Materials **611–612**, 425–435 (2014) https://doi.org/10.4028/www.scientific.net/KEM.611-612.425

[57] Crutzen, Y., Boman, R., Papeleux, L., Ponthot, J.-P.: Continuous roll forming including in-line welding and post-cut within an ALE formalism. Finite Elements in Analysis and Design **143**, 11–31 (2018) https://doi.org/10.1016/j.finel.2018.01.005

[58] Liang, Z., Liu, Y., Zou, T., Li, D., Ding, S., Xiao, H., Shi, L., Peng, Y.: Springback and longitudinal bow in chain-die forming U and hat channels. The International Journal of Advanced Manufacturing Technology **116**(11), 3571–3592 (2021) https://doi.org/10.1007/s00170-021-07374-y

[59] Kardes Sever, N.: Material characterisation for strength and formability limits of DP 1180 sheet. Canadian Metallurgical Quarterly **61**(3), 282–291 (2022) https://doi.org/10.1080/00084433.2022.2044687

[60] Deng, N., Korkolis, Y.P.: Elastic anisotropy of dual-phase steels with varying martensite content. International Journal of Solids and Structures **141**, 264–278 (2018) https://doi.org/10.1016/j.ijsolstr.2018.02.028

[61] Krajewski, S., Nowacki, J.: Mikrostruktura i właściwości stali o wysokiej wytrzymałości ahss. Welding Technology Review **83**(7) (2011)

[62] Meng, Z., Fang, Y., Ma, L.: A Method for Rapid Prediction of Edge Defects in Cold Roll Forming Process. Mathematics **9**(16), 1902 (2021) https://doi.org/10.3390/math9161902

[63] Skobir, D.A.: High-strength low-alloy (HSLA) steels. Materiali in tehnologije / Materials and technology **45**(4), 295–301 (2011)

[64] Shao, Y., Liu, C., Yan, Z., Li, H., Liu, Y.: Formation mechanism and control methods of acicular ferrite in HSLA steels: A review. Journal of Materials Science & Technology **34**(5), 737–744 (2018) https://doi.org/10.1016/j.jmst.2017.11.020

[65] ESB Group: HC380LA Cold Rolled Micro-Alloyed Steel. https://www.esb-group.com/en/products-din-en/cold-rolled-microalloyed-steel/hc380la-cold-rolled-micro-alloyed-steel/ Accessed 2025-05-28

[66] Geometrical Product Specifications (GPS) - Dimensional Measuring Equipment. Part 1: Design and Metrological Characteristics of Callipers. International Organization for Standardization (2019). www.iso.org

[67] Geometrical Product Specifications (GPS) - Acceptance and Reverification Tests for Coordinate Measuring Systems (CMS). Part 13: Optical 3D CMS. International Organization for Standardization (2021). www.iso.org

[68] BIPM, IEC, IFCC, ILAC, ISO, IUPAC, IUPAP, OIML: Evaluation of Measurement Data - Guide to the Expression of Uncertainty in Measurement (2008). https://www.bipm.org/documents/20126/2071204/JCGM_100_2008_E.pdf/cb0ef43f-baa5-11cf-3f85-4dcd86f77bd6

[69] Geometrical Product Specifications (GPS) - Inspection by Measurement of Workpieces and Measuring Equipment. Part 2: Guidance for the Estimation of Uncertainty in GPS Measurement, in Calibration of Measuring Equipment and in Product Verification. International Organization for Standardization (2011). www.iso.org

[70] Trombini, M., Maculotti, G., Maisano, D.A., Pagani, A., Franceschini, F.: Scaling photogrammetry: A comparative evaluation and metrological assessment across

small- and meso-scale domains. Precision Engineering **92**, 124–140 (2025) https://doi.org/10.1016/j.precisioneng.2024.12.002